Direct Observation of Nanorange Ordered Microporosity within Mesoporous Molecular Sieves

Jun Liu and X. Zhang*

Electron Microscopy Laboratory, School of Materials Science and Engineering, Tsinghua University, Beijing 100084, People's Republic of China

Y. Han and F.-S. Xiao

Department of Chemistry, Jilin University, Changchun 130023, People's Republic of China

Received November 17, 2001. Revised Manuscript Received March 13, 2002

Mesoporous molecular sieves SBA-15, and MAS-7 and MTS-9 synthesized from zeolite primary structure units, are characterized by high-resolution transmission electron microscopy (HRTEM). Direct observation of the micropores within these mesoporous materials via HRTEM is presented. And nanorange ordered microporosity is found for the first time within the pore walls of MAS-7 and MTS-9, which might be the key to the high hydrothermal stability of the mesoporous materials.

Introduction

Microporous zeolites are widely used catalysts, but they are incapable of converting large molecules because of the pore size limitation.[1,2] The crystalline nature endows them with high stability and the inherent pore size limitation of 1.3 nm.[1,2] On the other hand, mesoporous molecular sieves, such as MCM-41, are gaining interest for their potential applications in the separation and reactions involving large molecules.[3−8] However, its poor hydrothermal stability, which might be inherited from the amorphous nature,[9] has greatly limited the industrial application of MCM-41. Many efforts have been made to improve the stability of mesoporous molecular sieves,[10−12] such as by thickening or crystallizing the pore walls.[13−15] For example, SBA-15 with thicker pore walls has been synthesized as one of the most promising substitutes of MCM-41. SBA-15 exhibits much better hydrothermal stability[3,14] than MCM-41. Within the mesoporous silica SBA-15, existence of microporosity has been indirectly suggested by sorption isotherm measurements or calculation from small-angle X-ray scattering (SAXS) curves.[16−19] These micropores were estimated to be 0.5−1.5 nm in diameter.[18] It was proposed that materials with such a "bimodal pore system" (possessing both mesoporosity and microporosity) would be ideal as catalysts and adsorbents because molecules could be first transported through mesopore channels and then strongly adsorbed in micropores.[18]

Because most mesoporous materials are extremely vulnerable to heat and electron radiation, it is extraordinarily hard to obtain high-resolution transmission electron microscopic (HRTEM) images of mesoporous molecular sieves.[20] To our knowledge, direct evidence of microporosity within mesoporous molecular sieves has not been obtained yet. Recently, a mesoporous aluminosilicate (designated as MAS-7) with strong hydrothermal stability has been synthesized.[21] It can retain its highly ordered mesoporous structure even after the hydrothermal treatment of 100 h in boiling water according to our experimental results. Such a stable material could provide a possibility for studying mesoporous molecular sieves more directly and extensively.

* To whom correspondence should be addressed. Phone: 86-10-62773999. Fax: 86-10-62772507. E-mail: xzzhang@tsinghua.edu.cn.

(1) Davis, M. E.; Saldarriaga, C.; Montes, C.; Garces, J.; Crowder, C. *Nature* **1988**, *331*, 698.
(2) McCusker, L. B.; Baerlocher, C.; Jahn, A.; Bülow, M. *Zeolites* **1991**, *11*, 308.
(3) Kresge, C. T.; Leonowicz, M. E.; Roth, W. J.; Vartuli, J. C.; Beck, J. S. *Nature* **1992**, *352*, 710.
(4) Beck, J. S.; Vartuli, J. C.; Roth, W. J.; Leonowicz, M. E.; Kresge, C. T.; Schmitt, K. D.; Chu, C. T-W.; Olson, D. H.; Sheppard, E. W.; McCullen, S. B.; Higgins, J. B.; Schlenker, J. L. *J. Am. Chem. Soc.* **1992**, *114*, 10834.
(5) Zhao, D.; Feng, J.; Huo, Q.; Melosh, N.; Fredrickso, G. H.; Chmelka, B. F.; Stucky, G. D. *Science* **1998**, *279*, 548.
(6) Mokaya, R. Angew. *Chem. Int. Ed.* **1999**, *38*, 2930.
(7) Margolese, D.; Melero, J. A.; Christiansen, S. C.; Chmelka, B. F.; Stucky, G. D. *Chem. Mater.* **2000**, *12*, 2448.
(8) Newalkar, B. L.; Olanrewaju, J.; Komameni, S. *Chem. Mater.* **2001**, *13*, 552.
(9) Corma, A. *Chem. Rev.* **1997**, *97*, 2373.
(10) Ryoo, R.; Kim, J. M.; Shin, C. H. *J. Phys. Chem.* **1996**, *100*, 17718.
(11) Kim, S. S.; Zhang, W.; Pinnawaia, T. J. *Science* **1998**, *282*, 1032.
(12) Hwang, L. M.; Guo, W. P.; Deng, P.; Xue, Z. Y.; Li, Q. Z. *J. Phys. Chem. B* **2000**, *104*, 2817.
(13) Kloestra, K. R.; Bekkum, H. V.; Jansen, J. C. *Chem. Comm.* **1997**, 2281.
(14) Yang, P.; Zhao, D.; Margolese, D.; Chmelka, B. F.; Stucky, G. D. *Nature* **1998**, *396*, 152.
(15) Yang, P.; Zhao, D.; Margolese, D.; Chmelka, B. F.; Stucky, G. D. *Chem. Mater.* **1999**, *11*, 2831.
(16) Kruk, M.; Jaroniec, M.; Ko, C. H.; Ryoo, R. *Chem. Mater.* **2000**, *12*, 1961.
(17) Miyazawa, K.; Inagaki, S. *Chem. Comm.* **2000**, 2121.
(18) Göltner, C. G.; Smarsly, B.; Berton, B.; Antonietti, M. *Chem. Mater.* **2001**, *13*, 1617.
(19) Lukens, W. W.; Winkel, J. P. S.; Zhao, D.; Feng, J.; Stucky, G. D. *Langmuir* **1999**, *15*, 5403.
(20) Sakamoto, Y.; Kaeda, M.; Terasakl, O.; Zhao, D. Y.; Kim, J. M.; Stucky, G.; Shin, H. J.; Ryoo, R. *Nature* **2000**, *408*, 449.
(21) Han, Y.; Xiao, F. S.; Wu, S.; Sun, Y.; Meng, X.; Li, D.; Lin, S.; Deng, F.; Ai, X. *J. Phys. Chem. B* **2001**, *105*, 7963.

10.1021/cm0103951 CCC: $22.00
Published on Web 04/19/2002

In this paper, we report our HRTEM study on SBA-15 and MAS-7 and on MTS-9, a newly developed mesoporous titanosilicate with high catalytic activity.[21] Our HRTEM result directly confirms the existence of microporosity within the mesoporous molecular sieves. It presents, for the first time, an important finding of nanorange ordered micropores within the mesoscale pore wall of MAS-7 and MTS-9, which could be a strong indication of the existence of nanocrystallites. This would possibly reveal the key to the high hydrothermal stability of MAS-7 and MTS-9, resulting in the successful fabrication of highly stable materials with an ideal bimodal pore system, and thus pave the way for the commercial application of mesoporous materials.

Experimental Section

MTS-9 was synthesized in two steps: (1) The precursor solution with zeolite TS-1 primary structure units was prepared by mixing 6 mL of tetrapropylammonium hydroxide (TPAOH) aqueous solution (25%), 12 mL of H_2O, 0.3 mL of $Ti(OC_4H_9)$, and 5.6 mL of tetraethoxysilane (TEOS) under stirring ($TiO_2/SiO_2/TPAOH/C_2H_5OH/H_2O$ molar ratios of 1.0/30/8/120/1500). The mixture was then aged at 45 °C for 2−4 days. (2) Then, 0.8 g of $EO_{20}PO_{70}EO_{20}$ (Pluronic P123) was dissolved in 20 mL of H_2O/5 mL of HCl (10 mol/L), followed by 2.5 mL of precursor solution. The mixture was stirred at 40 °C for 20 h and then transferred into an autoclave for an additional reaction of 24 h at 100 °C. MAS-7 and SBA-15 were also prepared under similar conditions, as could be found in the Supporting Information.

After synthesis, the samples were dried in air and calcined at 550 °C for 5 h to remove the templates. The sample powder was then dispersed in dry ethanol and dropped onto the carbon microgrid for TEM observation.

TEM experiment was performed on a JEM-2010F electron microscope (JEOL, Japan) with a point resolution of 0.23 nm operated at 200 kV, which was equipped with a field emission gun and a Gatan image filter system (GIF 200, Gatan, United States). During the observation, care was taken not to damage the specimen, for the structures of the mesoporous molecular sieves could easily be destroyed by the electron beam. A small spotsize (Spotsize 3) was adopted, and the current density was restricted to below 9 pA/cm^2. Long exposure (2 min) of the specimen to the electron beam was carefully avoided, and adjustment of the instrument was carried out away from the specimen, and so forth. And we made sure that the specimen did not change significantly after photographing, so as to ensure that the sample had not been damaged. To reduce drifting, the part of the specimen strongly based on the supporting carbon and stretching out into the hole was selected for TEM observation.

X-ray diffraction patterns were obtained with a Siemens D5005 diffractometer, using Cu Kα radiation as a source. Sorption isotherms of nitrogen were measured at the boiling temperature of nitrogen with a micromeritics ASAP 2010 system, after the samples had been outgassed for 10 h at 300 °C. The mesopore size distribution was calculated with the Barret−Joyner−Halenda (BJH) model.[22]

Results and Discussion

The SBA-15 and MAS-7 samples we prepared both possess highly ordered mesoporous structures, as shown in Figures 1 and 2, respectively. This hexagonal periodicity extends all over the particles, usually several hundred nanometers in size. The Fourier diffractogram (Figure 1, inset) further confirms the strict hexagonal

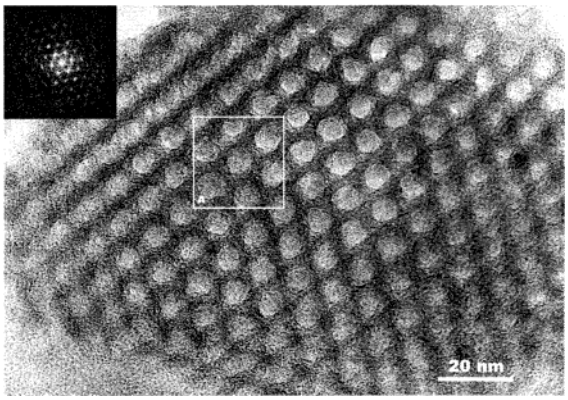

Figure 1. TEM image of SBA-15 and the corresponding Fourier diffractogram (inset). Area A is enlarged as Figure 5.

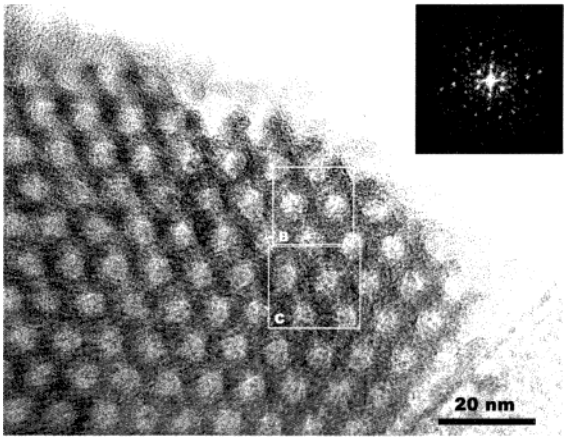

Figure 2. TEM image of MAS-7 and the corresponding Fourier diffractogram (inset). Area B and area C are enlarged as Figures 7 and 8, respectively.

structure of SBA-15 on mesoporous scale, which is in good agreement with previous reports.[3,5] MAS-7 also has a hexagonal mesoporous structure, with a weaker diffraction pattern (Figure 2, inset). However, the mesopores of MTS-9 are much less ordered (Figure 3), with the hexagonal pattern (Figure 3, inset) only discernible. This could probably result from the incorporation of heteroactoms (i.e., Ti or Al) into the mesoporous framework, as they are prepared under similar conditions. The mesoporous structures of these samples are also verified by the XRD results. And it should be noted that there were no distinguishable peaks in the wide-angle region of the XRD patterns, indicating that our products are of pure mesoporous phases without bulky zeolite crystals or metal oxides.[21]

Estimated from the bright contrast in Figure 1, the mesopores of SBA-15 are 6−8 nm in diameter, with a mean diameter of about 6.8 nm. The distances between neighboring mesopore centers range from 9 to 11 nm, with an average distance of ≈9.5 nm. This distance corresponds to the $d_{(100)}$ of ≈8.2 nm, measured from the Fourier diffractogram (Figure 1, inset). The pore wall thickness of SBA-15 is thus estimated to be ≈2.7 nm. All these are consistent with the XRD results and the pore size distribution calculations,[21] although the measurements would not be absolutely accurate. Due to the possible deviation of the pore channels from the incident electron beam and the difficulty in defining the edges of the pores, the pore size might have been underesti-

(22) Karlsson, A.; Stoker, M.; Schmidt, R. *Microporous Mesoporous Mater.* **1999**, *27*, 181.

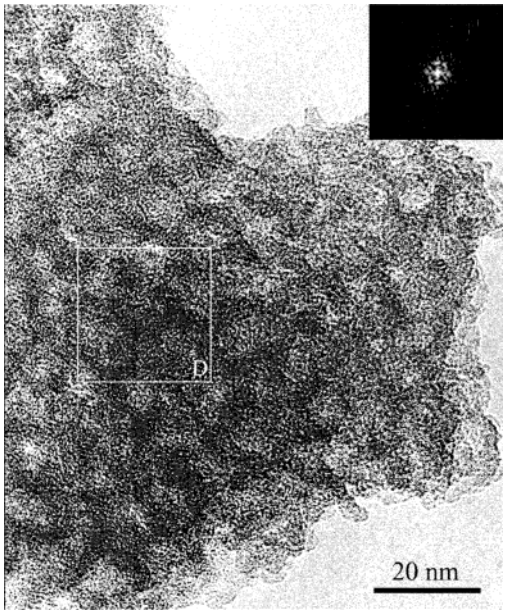

Figure 3. TEM image of MTS-9 and the corresponding Fourier diffractogram (inset). Area D is enlarged as Figure 9.

Table 1. Pore Sizes and Hydrothermal Stability of the Samples[a]

sample	distance between neighboring pore centers (nm)	mesopore size (nm)	Si/Al (or Si/Ti)[b]	hydrothermal stability[c] (h)
SBA-15	9−11	6−8	∞	60
MAS-7	9−11	6−8	30	100
MTS-9	12−14	7−8	40	100

[a] Pore sizes were measured from TEM images and the center distances were measured from the corresponding Fourier diffractograms. [b] Si/Al ratio for MAS-7, Si/Ti ratio for MTS-7, and either for SBA-15. [c] Hydrothermal stability was tested by the treatment of boiling water. The data listed in this column are the hours of treatment that the samples could maintain their mesoporous structures.

mated. However, this is the direct measurement that depends on no hypothesis or models. And the pore structure could be corroborated by the side view of the mesopore channels. Similarly, the mesoporous size and center distances of MAS-7 and MTS-9 were estimated from Figures 2 and 3 and are listed in Table 1.

In previous work, microporosity within SBA-15 was suggested by specific surface area calculation,[18] physisorption experiments,[16−18] and so forth. And the micropore diameter of 0.5−1.5 nm was indicated by calculation from small-angle X-ray scattering (SAXS) curves.[18] Nitrogen sorption isotherms of our samples are shown in Figure 4. Each of the curves present a steep slope at low relative pressure ($P/P_0 < 0.1$), similar to the results reported by others.[17,18] This is generally considered as a superposition of type I and type IV isotherms, indicating the existence of microporosity.[17,18,23] And t-plot analysis further confirms that a large volume of microporosity exists within MAS-7 (Figure 1S of the Supporting Information).

High-resolution transmission electron microscopy (HRTEM) was applied to study the microporosity within mesoporous materials directly. On the HRTEM image of SBA-15 (Figure 5), bright holes of ≈5 Å in diameter

(23) Gregg, S. J.; Sing, K. S. W. *Adsorption Surface Area and Porosity*; Academic Press: New York, 1982.

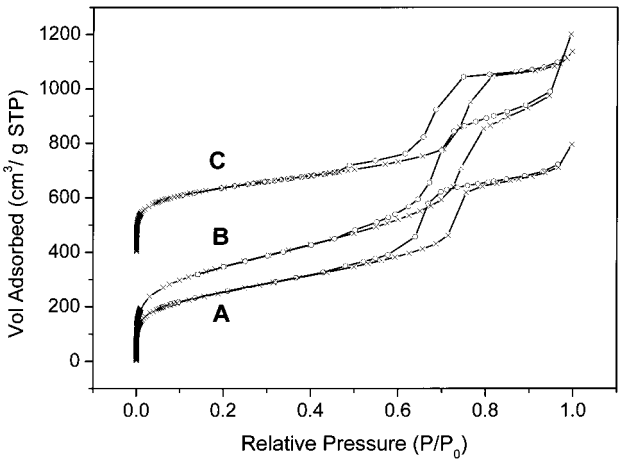

Figure 4. Nitrogen sorption isotherms of (A) SBA-15, (B) MTS-9, and (C) MAS-7.

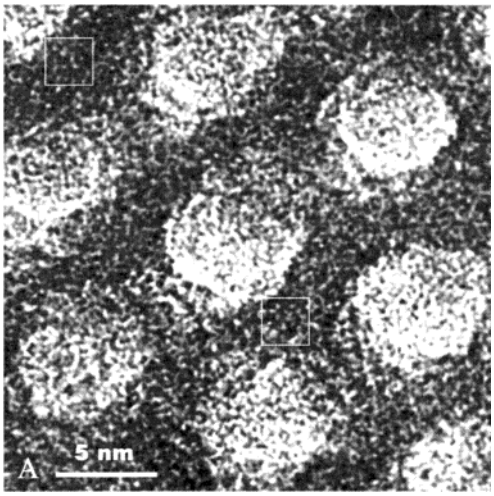

Figure 5. HRTEM image of SBA-15, corresponding to area A in Figure 1. The marked square areas present typical images of the micropores.

could be observed clearly, especially in those rectangular areas marked in Figure 5. During HRTEM observation, these bright contrasts did not change significantly as the defocus varied. Thus, they would not be confused with the atomic images, which change abruptly with defocus. Furthermore, the pore walls of our samples have been shown by XRD results to be basically amorphous in nature, which are unlikely to produce atomic resolution images. Therefore, we are convinced that these bright dots of ≈5 Å correspond to the mass-thickness contrasts that come from the micropores within the pore walls. To the best of our knowledge, this is the first direct evidence of the existence of microporosity within SBA-15. These micropores appear to be randomly distributed, just as hypothesized by the previous work.[15,18] And the pore sizes are similar to the previous estimation of other mesoporous molecular sieves.[19] Our measurements might not be accurate due to some overlaps of the micropores and the difficulty in defining the edges. However, the existence of micropores smaller than 1 nm in diameter has been apparently substantiated. It is notable that a mesoporous system with such tiny micropores in the walls might not tally with most models currently used. This could be a considerable contribution to the difference of specific surface area between calculation and experiments.

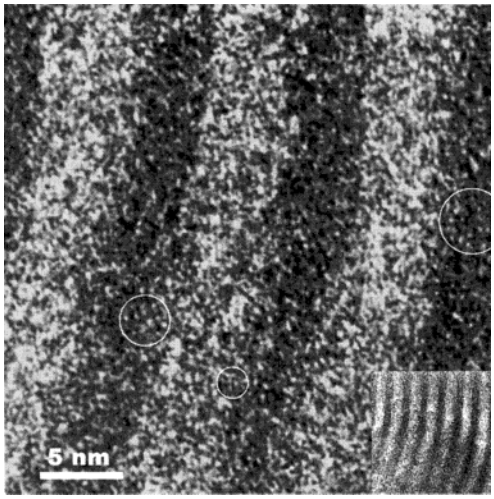

Figure 6. HRTEM image as the side view of SBA-15. Inset is the image at smaller magnitude to show the mesoporous structure. The marked circular areas present typical images of the micropores.

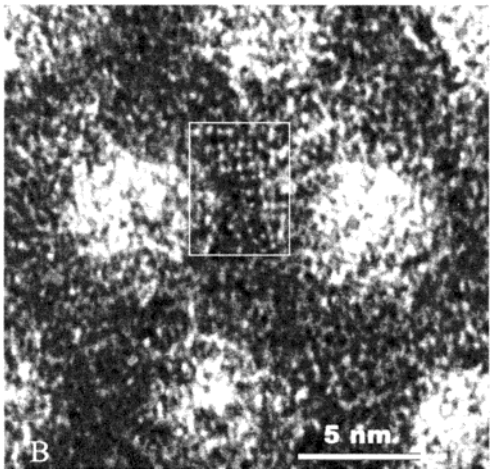

Figure 7. HRTEM image of MAS-7, corresponding to area B in Figure 2. The rectanglar area presents fairly ordered micropore arrays.

Figure 6 shows the side view of the mesopore channels in SBA-15, the photograph taken perpendicular to the channels. Accordingly, the bright channels in Figure 6 correspond to the mesopores, about 6.8 nm in width. Figure 6 is designed to study the shape or direction of the micropores. If the micropores are one-dimensional (1D) in shape, 1D channels would be observed in Figure 5 and/or Figure 6, as they are taken from perpendicular directions. However, the circular bright holes of ≈5 Å similar to those in Figure 5 are also observed in Figure 6. This suggests that the micropores are approximately spherical cages rather than cylindrical channels. Again, the micropores are found randomly distributed.

Figures 7 and 8 are HRTEM images of MAS-7, and both of them clearly show some micropores ≈4 Å in diameter. This further confirms the presence of microporosity within such mesoporous materials prepared from triblock copolymer templates. What is more important is that within the mesoscale pore walls, micropore arrays with more or less periodicity are found (especially in those areas marked with circles or rectangles in Figures 7 and 8). These micropore arrays are mostly around 2 nm in size (marked areas in Figure 8).

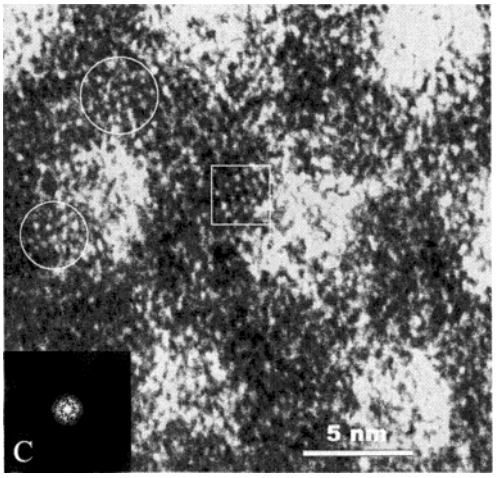

Figure 8. HRTEM image of MAS-7, corresponding to area C in Figure 2. Inset is the Fourier diffractogram of the square area. Other areas marked with circles present fairly ordered micropore arrays.

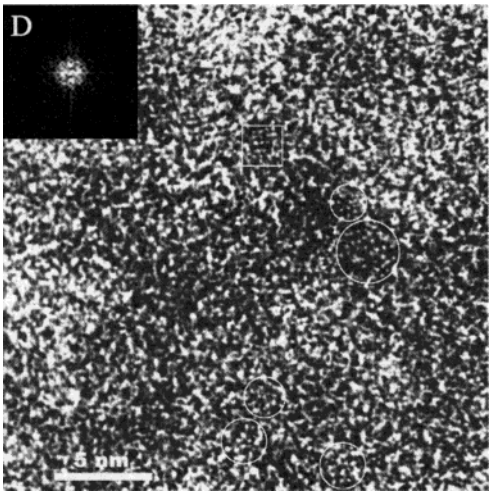

Figure 9. HRTEM image of MTS-9, corresponding to area D in Figure 3. Inset is the Fourier diffractogram of the square area. Other areas marked with circles present fairly ordered micropore arrays.

The Fourier diffractogram (Figure 8, inset) corresponding to the micropore array presents a discernible hexagonal diffraction pattern, which convincingly confirms the existence of nanorange hexagonally ordered microporosity within the pore walls of MAS-7. To our knowledge, this has not been reported yet. In a MTS-9 molecular sieve, which was also prepared using zeolite primary structure units, similar micropores could also be found (as shown in Figure 9). This further confirms the existence of micropore nanoarrays and also suggests that the zeolite structure units might be the origin of these micropores because both MAS-7 and MTS-9 were prepared from precursors containing zeolite nanoclusters.

Microporous zeolites are known to be hydrothermally stable. Thus, good stability could be expected for these mesoporous materials prepared from zeolite structure units and containing micropore nanoarrays. MAS-7 and MTS-9 both exhibit excellent stability, even significantly better than SBA-15 (Table 1). They can maintain the mesoporous structure even after 100 h of treatment in boiling water, which is 40 h better than that of SBA-15. Since MAS-7, MTS-9, and SBA-15 were all prepared

under similar conditions, and both MAS-7 and MTS-9 possess micropore nanoarrays, whereas SBA-15 does not, their strong hydrothermal stability might result from the nanoranged ordered micropore structures. These microporous structures exist in MAS-7 and MTS-9, which were both prepared from zeolite structure units and both exhibit high hydrothermal stability. Therefore, the nanorange ordered micropore structure might play a role similar to that of the zeolite crystallites in improving hydrothermal stability. Or they could be a strong indication of the existence of nanocrystallites in MAS-7 and MTS-9. There could be some other factors that contribute to this stability, however, such as the thicker pore walls.[21] The catalytic activities of SBA-15, MAS-7, and MTS-9 have been discussed in ref 21. MAS-7 and MTS-9 show much better catalytic activities than other mesoporous materials such as Al−SBA-15, H−ZSM-5, and Ti−SBA-15.[21] It appears that the bimodal pore system and the nanorange ordered microporosity are advantageous for catalysts and adsorbents, though further research is needed.

Conclusion

The existence of microporosity within the mesoporous molecular sieves of SBA-15, MAS-7, and MTS-9 has been directly confirmed by TEM images. The micropores are found to be spherical cages in shape and about 0.5 nm in diameter. Nanorange ordered microporosity was found for the first time within mesoscale pore walls of the MAS-7 and MTS-9, which had been synthesized from zeolite primary structure units, and both exhibit significantly higher hydrothermal stability and catalytic activity than SBA-15. This might be the first step toward the fabrication of crystalline mesoporous materials with high hydrothermal stability. And the relation between the microporosity, crystallization, and hydrothermal stability of mesoporous materials is still to be investigated.

Supporting Information Available: Detailed preparation processes and t-plots of MAS-7 and SBA-15 (PDF). This material is available free of charge via the Internet at http://pubs.acs.org.

Note Added after ASAP Posting

This article was released ASAP on 4/19/2002 with a minor error in the referencing. The correct version was posted on 5/14/2002.

CM0103951